OPEN ACCESS
11th International Conference on New Frontiers in Physics
(ICNFP 2021)
International Journal of Modern Physics: Conference Series
Vol. 51 (2023) 2361013 (16 pages)

DOI: 10.1142/S201019452361013X

Upgrade of the BM@N detector for studies of heavy ion interactions

Anna Maksymchuk
Joint Institute for Nuclear Research, 141980 Dubna, Russia
maksymchuk@jinr.ru

Alexandre Vishnevskiy
Joint Institute for Nuclear Research, 141980 Dubna, Russia
alex.vishnevskiy@mail.ru

Dmitrii Dementev
Joint Institute for Nuclear Research, 141980 Dubna, Russia
dementiev@jinr.ru

Fedor Guber
Institute for Nuclear Research, 117312 Moscow, Russia
guber@inr.ru

Mikhail Kapishin
Joint Institute for Nuclear Research, 141980 Dubna, Russia
kapishin@jinr.ru

Yuri Murin
Joint Institute for Nuclear Research, 141980 Dubna, Russia
murin@jinr.ru

Semen Piyadin
Joint Institute for Nuclear Research, 141980 Dubna, Russia
piyadin@jinr.ru

Hans Rudolf Schmidt
GSI Helmholtzzentrum für Schwerionenforschung, 64291 Darmstadt, Germany
Physics Institute, University of Tuebingen, 72076 Tuebingen, Germany
h.r.schmidt@gsi.de

Peter Senger
GSI Helmholtzzentrum für Schwerionenforschung, 64291 Darmstadt, Germany
National Research Nuclear University MEPhI, 115409 Moscow, Russia
p.senger@gsi.de

Nikolai Zamyatin
Joint Institute for Nuclear Research, 141980 Dubna, Russia
nzamiatin@mail.ru

Alexander Zinchenko
Joint Institute for Nuclear Research, 141980 Dubna, Russia
alexander.zinchenko@jinr.ru

Published 27 December 2023

In the next years the Baryonic Matter at Nuclotron (BM@N) experiment at Joint Institute for Nuclear Research (JINR) will carry out the physics program with heavy ion beams with energies up to 3.9 AGeV and intensities up to $2 \cdot 10^6$ ions/s. The experiment is devoted to measure observables sensitive to the equation of state of dense baryonic matter. To meet this goal the existing BM@N set-up will be upgraded with fast hybrid tracking system, which includes beam tracking detectors, a large aperture silicon tracking system, gas electron multiplier stations and cathode strip chambers. The measurement of the event plane and centrality will be achieved with a forward hadron calorimeter and granular hodoscopes. The physics program and configuration of the upgraded BM@N set-up are presented.

Keywords: Heavy-ion collisions; new experimental facilities; nuclear matter equation-of-state.

PACS numbers: 25.75.-q, 29.40.Gx, 21.80.+a, 21.65.+f

1. Introduction

Theoretical and experimental investigations of the strongly interacting matter properties at high temperatures and densities are among the most exciting research programs of modern high-energy nuclear physics. The recent astronomical observations of supermassive neutron stars and neutron star mergers challenge our knowledge on high-density quantum chromodynamics (QCD) matter, like its equation-of-state (EOS) and its microscopic degrees-of-freedom at high baryon densities. Future measurements of mass and radius of neutron stars and the precise spectroscopy of gravitational waves will improve our understanding of the high-density EOS. Complementary information will be obtained by laboratory experiments with energetic heavy-ion collisions, which provide the opportunity to investigate both the EOS at high density and to explore the degrees-of-freedom of this matter, including the search for new phases of high-density matter, which possibly feature characteristic structures like critical points. The investigation of the QCD phase diagram is a worldwide endeavor undertaken at heavy-ion accelerators like LHC and SPS at CERN, RHIC at BNL, and SIS18 at GSI. Future projects, like the Facility for

Antiproton and Ion Research (FAIR) in Germany,[1] and the Nuclotron-based Ion Collider Facility (NICA) in Russia,[2] will open unique possibilities to produce and explore QCD matter at densities, which are predicted to exist in the core of neutron stars. In particular, the fixed-target Compressed Baryonic Matter (CBM) experiment at FAIR,[3] and the Multi-Purpose Detector (MPD) at the NICA collider[4] will focus on the investigation of diagnostic probes which are sensitive to the EOS and the degrees-of-freedom of high-density QCD matter. The existing BM@N experiment[5] will be upgraded in order to investigate heavy-ion collisions at beam energies up to about 4 AGeV, where the fireball is predicted to be compressed to about 4 times the saturation density.

2. BM@N Heavy Ion Physics Program

The future Nuclotron beams are well suited to produce dense nuclear matter in the collisions of heavy nuclei. In central Au + Au collision at top Nuclotron beam energies, densities of 4–5 times saturation densities will be reached in the center of the reaction volume,[6] which corresponds to the densities prevailing in the core of neutron stars. Like matter in compact stellar objects, the matter in this fireball will be compressed according to the EOS, and experiments at the Nuclotron may shed light on the properties of neutron stars. These laboratory experiments complement astronomical observations of mass and radii of neutron stars, in order to determine the high-density EOS. Laboratory measurements, however, might be also sensitive to the degrees-of-freedom of dense nuclear, which are expected to change with increasing density, when the nucleons overlap and start to melt into their elementary constituents. Moreover, heavy-ion experiments may also provide information on the role of hyperons in neutron stars.

2.1. *The nuclear-matter equation-of-state*

The nuclear matter equation-of-state (EOS) relates thermodynamic properties like pressure, volume, temperature, etc., and can be written as the energy per nucleon as a function of density:

$$E_A(\rho, \delta) = E_A(\rho, 0) + E_{Sym}(\rho) \cdot \delta^2 + O(\delta^4) \quad (1)$$

where the first term represents the EOS for symmetric matter, and the second term is the symmetry energy with $\delta = (\rho_n - \rho_p)/\rho$ the isospin asymmetry parameter. The EOS of symmetric matter is commonly parameterized by the binding energy per nucleon at saturation density ρ_0 and the incompressibility K_{nm}, which corresponds to the curvature around ρ_0. Experiments at GSI have been performed by the FOPI collaboration, which measured the elliptic flow of protons, deuterons, tritons, and ^{3}He in Au + Au collisions at beam kinetic energies between 0.4 and 1.5 AGeV.[7] The elliptic flow of particles is driven by the pressure gradient in the

reaction volume, and, therefore, is sensitive to the EOS. The FOPI data have been interpreted by calculations using the isospin-dependent quantum molecular dynamics (IQMD) transport code.[7] It was found, that the data can be explained assuming a nuclear incompressibility of $K_{nm} = 190 \pm 30$ MeV, which corresponds to a soft EOS for symmetric nuclear matter up to nuclear densities of about 2–3 ρ_0. In order to contribute to our understanding of neutron stars, densities of 4–5 ρ_0 have to be produced and investigated. Even higher densities have been reached in experiments at the AGS in Brookhaven, which measured both the directed and the elliptic flow of protons in Au + Au collisions at energies between 2 and 11 AGeV.[8] It turned out, that the data on directed flow agree with the assumption of a soft EOS, whereas the elliptic flow data point towards a hard EOS.[9] In conclusion, the interpretation of these data did not much constrain the range of possible EOS at high densities, and one important goal of the BM@N research program is to improve these flow measurements. An alternative approach to study the EOS of symmetric matter is to investigate subthreshold strangeness production in heavy-ion collisions. This method has been pioneered by the KaoS collaboration at GSI, which measured the excitation function of K^+ meson production in Au + Au and C + C collisions at beam energies from 0.8 and 1.5 AGeV.[10] Please note, that the minimum energy to create a K^+ meson in nucleon-nucleon collisions, for example via the process p + p$\rightarrow$ $K + \Lambda$p, is 1.58 GeV. Therefore, at sub-threshold energies, strangeness has to be produced via multiple collisions involving pions and Delta resonances. These sequential collisions occur more frequently, if the baryon density is high, which means, that the EOS is soft. The EOS effects show up in the heavy Au + Au system, but are be less pronounced in the small C + C system. The kaon yield ratio from Au + Au over C + C collisions clearly exhibits an enhancement towards lower beam energies, which is caused by a soft EOS with a nuclear incompressibility of $K_{nm} \approx 200$ MeV according to RQMD and IQMD transport calculations.[11,12] This result agrees with the elliptic flow measurements done by FOPI in the same energy range, covering baryon densities up to about twice saturation density. Another very promising observable sensitive to the high-density EOS of symmetric matter is the excitation function of multi-strange (anti-)hyperons. According to transport models, Ξ and Ω hyperons are produced in sequential collisions involving kaons and Λ hyperons, and, therefore, are sensitive to the density in the fireball.[13,14] This sensitivity is expected to increase at beam energies close to or even below the production threshold. For example, the production of a Ξ^- hyperon in a proton-proton collision p + p$\rightarrow$ $\Xi^- K^+ K^+$ p requires a minimum proton energy of $E_{thr} = 3.7$ GeV. Nevertheless, Ξ^- hyperons can be produced in heavy-collisions via strangeness exchange reaction at energies above the lambda threshold of 1.6 GeV via lambda-lambda collisions $\Lambda^0\Lambda^0 \rightarrow \Xi^-$p. Even Ω hyperons can be produced, when the Ξ collides with another lambda $\Lambda^0\Xi^- \rightarrow \Omega^-$n or with a kaon $K^-\Xi^- \rightarrow \Omega^-\pi^-$. Therefore, the measurement of multi-strange hyperons will be a central goal of the BM@N research program at the Nuclotron.

2.2. *Mixed phases of QCD matter*

In central Au + Au collisions at top Nuclotron beam energies, baryon densities of more than 4–5 ρ_0 might be reached. At these densities, the nucleons may already partly overlap, and start to melt into their elementary constituents. The question is, which observable might be sensitive to this onset of deconfinement? At very high bombarding energies like at LHC, there is experimental and theoretical evidence for the creation of a deconfined phase, the so-called Quark-Gluon-Plasma (QGP). One of the arguments is, that the yield of all created hadrons can be perfectly explained by the statistical hadronization models, assuming chemical equilibrium in a fireball with a temperature of about 156 MeV and vanishing baryon-chemical potential.[15] In particular the observation, that also multi-strange (anti-) hyperons are equilibrated, although their scattering cross section with nucleons is small, has been interpreted as indication for a phase transition from partonic to hadronic matter, which drives the hyperons into equilibration.[16] The same observation was made for Pb + Pb collisions at a beam kinetic energy of 30 AGeV at the SPS for a fireball temperature of 138 MeV and a baryon-chemical potential of 380 MeV.[17] At much lower beam energies, i.e. in Ar + KCl collisions at an energy of 1.76 AGeV, most of the hadron yields are also compatible with the statistical model for a temperature of 76 MeV and a baryon-chemical potential of 800 MeV. The yield of Ξ^- hyperons, however, exceeds the model prediction by about a factor 24 ± 9.[18] This high yield is generated by multiple collisions including strangeness exchange reactions in a hadronic environment, as discussed above. Obviously, the Ξ^- hyperons did not equilibrate, because the beam energy is too low to for a phase transition. The energies at the Nuclotron might be sufficiently high to see the onset of deconfinement. Therefore, the BM@N research program includes the measurement of the excitation function of multi-strange hyperons in Au + Au collisions in order to explore the onset of equilibration of multi-strange hyperons at high net-baryon densities.

2.3. *Hyperons in dense nuclear matter*

The role of hyperons in neutron stars is still a puzzle. If the hyperon chemical potential in dense nuclear matter falls below the chemical potential of neutrons and protons, these particles will decay in to hyperons. This process is expected to occur in the core of neutron stars at densities above 4–5 ρ_0, leading to a softening of the nuclear equation-of-state, and, hence, preventing the existence of high mass neutron stars. On the other hand, neutron stars with about twice the mass of our sun have been observed.[19] The hyperon chemical potential depends not only on the repulsive two-body hyperon-nucleon ΛN force, but also on the three-body repulsive ΛNN interaction, which becomes increasingly important at high densities.[20] Therefore, laboratory experiments devoted to the investigation of hyperon-nucleon interactions will shed light on the role of hyperons in neutron stars. One possibility to study these interactions is to discover new hypernuclei and to measure their

lifetimes. According to statistical model and transport calculations, light hypernuclei and even double-lambda hypernuclei are abundantly produced in heavy-ion collisions at Nuclotron and NICA energies.[21,22] This opens the opportunity for the upgraded BM@N experiment, to measure light hypernuclei in Au + Au collision at the top Nuclotron beam energy, and to contribute to the solution of the long-standing hyperon puzzle in neutron stars.

3. BM@N Detector

BM@N is the first experiment at the accelerator complex of NICA Nuclotron. The aim of the BM@N experiment is to study interactions of relativistic heavy ion beams with fixed targets.[23] The Nuclotron will provide verity of beams from protons to gold ions with the kinetic energy of ions ranging from 1 to 6 GeV per nucleon. The maximum kinetic energy for ions with the ratio of the charge to the atomic weight Z/A of 1/2 is 6 GeV per nucleon. The maximum kinetic energy for heavy ions with the ratio of Z/A $\sim$ 1/3 is 4.5 GeV per nucleon. The maximum kinetic energy of protons is 13 GeV. The requirements for detector subsystems are very high, as all physical measurements will be performed under conditions of high beam intensities in collisions with large multiplicity of charged particles. The scheme of the BM@N detector configuration for heavy ion program is shown in Fig. 1.

The experiment combines high precision track measurements with time-of-flight information for particle identification. The magnetic field of the analyzing magnet can be varied up to 1 T to get the optimal detector acceptance and momentum resolution for different reactions and energies of the beam. The vertical gap between the poles of the analyzing magnet available for the detector installation is about

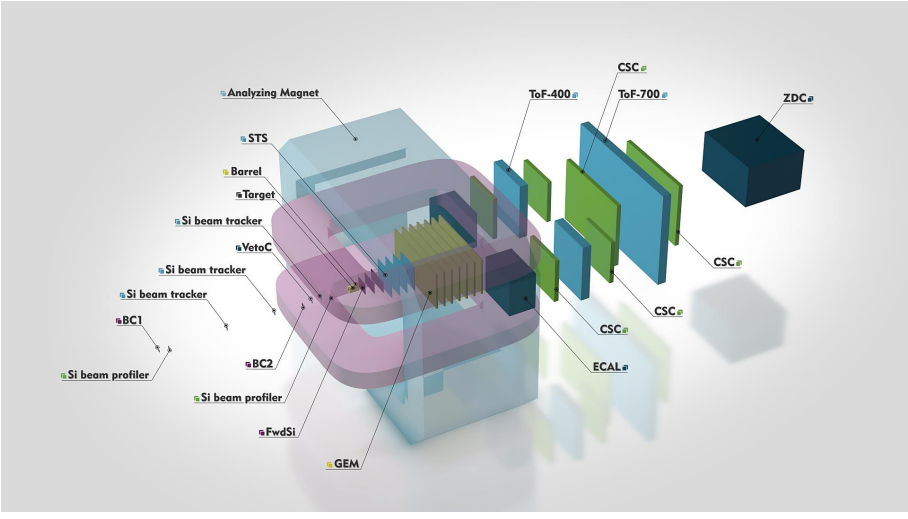

Fig. 1. Schematic view of the BM@N setup for the heavy ion program (without vacuum beam pipe).

1 m. A wide-aperture central tracking system is based on seven planes of triple gas electron multipliers (GEM). Detectors of this kind are operational at high radiation loadings and in strong magnetic fields.[24] Central tracking system is located downstream the target inside the analyzing magnet. The momentum of charged particles — the products of interactions of the beam with the target — are measured by the curvature of their trajectories in a magnetic field. To eliminate a systematic shift of the reconstructed tracks in the magnetic field, GEM detectors are oriented in alternating order so that the electric field for the neighboring planes has opposite directions. Double-sided silicon micro-strip detectors (FwdSi, STS) are installed between the target and the central tracking system to determine the interaction vertex with high accuracy and to improve the precision of track reconstruction, especially in the region of small particle momentum. The outer tracking system consists of six planes of Cathode Strip Chambers (CSC). It is situated outside the magnetic field and is intended to precise parameters of tracks, obtained in GEM detectors inside the analyzing magnet, and thus to increase the efficiency of track reconstruction. Beside improvement of particles momentum identification, refined track in CSC is used to find corresponding hit in the ToF-400 and ToF-700 time-of-flight systems. The design parameters of the time-of-flight detectors based on a multi gap resistive plate chamber (mRPC) technology with a strip read-out allows one to perform separation between hadrons (π, K, p) as well as light nuclei with the momentum up to few GeV/c. The Zero Degree Calorimeter (ZDC) detector is foreseen for the analysis of the collision impact parameter by measuring the energy of the fragments of colliding particles. The Barell detector placed around the target and partially overlapping the backward hemisphere is planned to generate a trigger signal for the DAQ. A starting signal for the ToF400 and ToF700 detectors will be generated by the Beam Counter (BC2). A vacuum beam pipe will be integrated into the experimental setup to minimize the amount of scattering material on the way of heavy ions (it is not shown in Fig. 1). Groups of trigger detectors and beam profile meters will be installed inside the beam pipe in vacuum boxes. Three silicon beam trackers will determine the trajectory of the beam particles before the target. The targets will be installed inside the target station. The target station will allow changing three different types of targets for data taking and one empty target for background evaluation without breaking the vacuum.

Main detector subsystems to be integrated into upgraded BM@N experimental setup are described below.

3.1. *Forward silicon detectors*

Forward silicon detectors (FwdSi) are installed between the target and the GEM central tracking system to increase the tracking efficiency and improve the precision of the primary vertex reconstruction. FwdSi consist of three planes combined from two half planes. Each half-plane has a hole for a beam pipe, inlet and outlet for the cooling system (cold dry air), and cross-boards for connection with the DAQ

system and power supply. The total number of modules in planes is 42. A silicon detector module consists of two DSSDs, which are wire bonded strip to strip. The detector sensitive volume is $63 \times 63 \times 0.3$ mm^3. The pitches for the P-side and N-side are 95 and 103 μm, respectively. Stereo angle between strips is 2.5 degrees, number of strips for each side – 640. Total sensitive area of the FwdSi is ~ 0.3 m^2. Since detector does not have integrated capacitors, pitch adapter (PA) is used to electrically decouple the DC current from the electronic inputs. PA has two different topologies for each DSSD side. Each PA has 640 channels, value of poly-Si resistor is about 1 MOm, value of integrated capacitor is 120 pF, capacitor working voltage is 100 V and breakdown voltage more than 150 V. After PAs signal from detector transfer to VATAGP7.1 ASICs manufactured by IDEAS, Norway (5 chips per module side). The main ASIC parameters are 128 input channels, multiplexed output and dynamic range $\pm$ 30 fC.

3.2. *Silicon tracking system*

The Silicon Tracking System (STS) of the BM@N consists of four stations equipped with 292 double-sided micro-strip silicon sensors providing information on the position, time and energy released by the particle passing through a sensor of the STS. The STS configuration is described in details in Ref.25. STS sensors of two sizes are used: 42 mm $\times$ 62 mm, and 62 mm $\times$ 62 mm. The sensors have a thickness of 320 $\pm$15 μm. Each sensor has 1024 strips on each side with a strip pitch of 58 μm. Strips on the N-side of the sensor are straight, while the strips on the P-side are titled at an angle of 7.5 degree relative to the strips on the opposite side. Short angled strips located on both edges are connected via a second metallization layer on the P-side. The 2048 strips of each sensor (P and N side) are readout simultaneously by 16 ASICs sitting on 2 Front-End Boards (FEBs). Each ASIC is connected to the sensor via 2 low-mass aluminumpolyimide micro-cables, each reading out 64 strips. The unit consisting of a sensor, 32 cables and a FEB is called a module. Several modules are mounted on ultralight spaceframes, the trusses, made of high modulus carbon fiber. This super module, consisting of up to 10 modules with readout micro-cables transmitting the signals in both directions (up and down), is the so-called ladder. The stations 1, 2, 3, and 4 comprise 24, 52, 64, and 104 modules, respectively, with sensors of size 62×62 mm^2. In the inner part of each station, 8 modules with sensors of size 42×62 mm^2 are located. Four modules with central sensors of size 42×62 mm^2 with cut edges cover the space close to the beam pipe, in order to detect the particles emitted at the smallest scattering angles. The first station is located 30 cm downstream the target. The distance between all STS stations is 20 cm. The sensors on the ladders are tiled with an overlap of 1.3 mm to cover the existing 1 mm wide dead area at the edges of the sensors. The data acquisition chain of the BM@N STS conceptually exploits the free-streaming readout scheme being developed for the CBM.[26] The frontend electronics of the STS is an integral part of the module that relies on the STS-XYTER ASIC developed by the CBM

collaboration. Each ASIC provides 128 channels operating in a self-triggered mode. The ASIC provides a 5 bits amplitude and 14 bits time stamp information for each hit frame. The ASICs communicate with the system through the configurable multichannel e-link protocol. The maximum hit rate per one channel in the BM@N STS setup is $\sim$ 20 kHz/channel.

3.3. *Central tracking system*

Central tracking system of BM@N experiment is based on triple GEM detectors. Production and assembly processes of the large size (up to 2m long) GEM-based detectors are well developed at CERN Micro-Pattern Technologies Workshop. Since non-glue foil-stretching technology is involved, one chamber can be assembled in several hours and easily re-opened for technical service if needed. Triple-GEM configuration performs low probability of discharge propagation and stable operation at gains above 10^5. Detectors are operational at magnetic field up to 1.5 T. For this reason, two coordinate triple GEM detectors were chosen for the central part of the BM@N tracking system. BM@N GEM detectors consist of three multipliers, with a drift gap of 3 mm, first transfer gap of 2.5 mm, second transfer gap of 2 mm and an induction gap of 1.5 mm. Two-coordinate readout of the signal is done by the sets of parallel metal strips on the anode readout board. The inclination angles of bottom layer strips (X coordinate) and top layer strips (Y coordinate) to the vertical are 0 and 15 degrees, respectively. X and Y strip widths are 680 and 160 μm. The strip pitch is 800 μm for both layers. Groups of 128 strips are connected to the inputs of the front-end ASIC via a connector on the readout board. The BM@N GEM tracking system final configuration consists of two types of the GEM chambers: seven with active area 1632 $\times$ 450 mm^2 and seven with active area 1632 $\times$ 390 mm^2, combined in seven planes. Due to the large multiplicity near the beam line, readout layer is divided into outer and inner zones for both types of detectors. GEM front-end electronics is based on the charge sensitive pre-amplifier chip VA163 manufactured be IDEAS, Norway (4 chips per front-end-card). The chip has 32 channels. Each channel contains a charge-sensitive preamplifier, a shaper with 0.5 μs peaking time and a sample-hold circuit. An analog multiplexer with 32 inputs allows one to perform serial read-out channel by channel. The chip can be used to amplify and read negative and positive charges in the range from -1.5 pC to $+1.5$ pC. More fast front-end-electronics based on VMM3a chips is currently under development.

3.4. *Outer tracking system*

For the heavy ion beam program, a set of cathode strip chambers (CSC) will replace existing drift chambers, which were used in runs with light ions as outer tracking system. The full configuration of the outer tracking system for heavy ion program will consist of four planes of 1129 $\times$ 1065 mm^2 CSC and two planes of 2190 $\times$ 1453 mm^2 CSC.[27] The CSC detectors are situated outside the magnetic field with the aim

to make precise link to the tracks, reconstructed in the GEM detectors inside the analyzing magnet. Tracks refined in CSC are used to improve particles momentum reconstruction and to find corresponding hits in the time-of-flight systems ToF400 and ToF700. Each CSC detector consists of an anode plane located between two cathode planes. The anode plane is a set of gilded tungsten wires with the diameter of 30 μm which are fixed on the plane with a step of 2.5 mm. The gap between the anode plane and each cathode plane is 3.5 mm. There is a spacer between the cathode planes to prevent deformation of the chamber due to the gas pressure inside. The anode wires are supported by two special wires strained across in the middle. Both cathode planes are made from PCBs (printed circuit boards). A two-coordinate readout of the signal is performed on two cathode boards using sets of parallel metal strips. The inclination angles of the cathode strips to the vertical axis are 0 degrees (X coordinate) and 15 degrees (Y coordinate). The pitch of the X and Y strips is 2.5 mm. PCBs are glued to the support honeycomb. Due to the a large multiplicity of charged particles in Au-Au collisions, readout layer is divided into outer (cold) and inner (hot) zones. CSC front-end-electronics is based on the VA163 chip (same with GEMs).

3.5. *Forward hadron calorimeter*

A new forward hadron calorimeter (FHCal) will be served as a Zero Degree Calorimeter (ZDC) at the BM@N setup. It will be used to measure the centrality and reaction plane orientation in heavy ion experiments. The calorimeter is positioned at the end of the BM@N setup at a distance 9 m from the target. It has modular structure in the transverse plane and consists of 54 individual modules. The inner part of FHCal consists of 34 modules with transverse sizes of $15 \times 15\ cm^2$. There is the beam hole in the center with transverse size $15 \times 15\ cm^2$. This hole is required to reduce the radiation dose and activation of the calorimeter and to reduce the neutron background at the rear part, where the photodetectors and electronics are located. The inner modules have a length equal to 4 nuclear interaction lengths. The outer part consists of twenty modules with transverse dimensions of $20 \times 20\ cm^2$ and a length equivalent to about 5.6 nuclear interaction lengths. All FHCal modules have sampling structure. The outer modules have 60 lead/scintillator layers, while the inner modules have 42 similar layers. Each layer consists of 16 mm lead plates and 4 mm scintillator plates. The light from each scintillator plate is transported to the end of modules with WLS-fiber embedded in the groove in the plate. The fibers of each six consecutive scintillator tiles are combined to one optical connector and light from these 6 fibers is read-out with single photodetector (Hamamatsu MPPC with active sensitive area $3 \times 3\ mm^2$) mounted on front-end electronics plate at the end of the module. Such longitudinal segmentation provides the uniformity of the light collection along the module and high dynamic range of the calorimeter response. The segmentation of modules also allows to perform the FHCal energy calibration with cosmic muons. The presence of a beam hole in the calorimeter leads

to a significant leakage of heavy fragments through this hole and, as a consequence, to a non-monotonic dependence of the deposited energy in the calorimeter on the collisions centrality. To solve this problem a nuclear fragment hodoscope (FQH) will be used to measure the charges of heavy fragments. The FQH consist of 16 quartz plates 160 mm long, 4 mm thickness and 10 mm width. The active area of the hodoscope is 160 $\times$ 160 mm^2. The light from each of the 16 quartz plates is readout from two opposite ends by two pairs of Hamamatsu photodiodes MPRS S12572-015P with an active region size of 3 $\times$ 3 mm^2 and a quantum efficiency of about 20%. To extend forward calorimeter system the scintillator wall (ScWall) detector will be used to have the possibility to measure not only the centrality and reaction plane in heavy ion collisions but also the fragmentation of nucleus. The ScWall consists of 36 scintillator detectors with transverse sizes 7.5 $\times$ 7.5 cm^2 surrounding the beam hole and 134 outer cells with transverse sizes 15 $\times$ 15 cm^2. The light from each scintillator detector is collected by WLS glued in the groove in the scintillator plate and will be detected with 1 mm^2 Hamamatsu MPPC.

4. Stages of BM@N Experimental Setup Upgrade

In the initial stages the BM@N experiment was used to measure reactions with low-intensity beams of light ions, which traversed the setup in the air without the beam pipe. Main detector subsystems were present in a limited configuration. The outer tracking system consisted of two drift chambers on both sides of ToF-700. But after the final upgrade of the set-up and the Nuclotron, intensity of the Au ion beam at BM@N is planned to be few 10^6 ions/s. In Table 1 different stages of BM@N experimental set-up upgrade are described.

In Fig. 2 the interaction rates are presented for different experiments with heavy ion collisions at different energies per nucleon-nucleon collision in the center of mass system. The beam energy of the BM@N experiment is in the intermediate range between experiments at the SIS-18 and NICA/FAIR facilities and partially overlaps

Table 1. Beam parameters and setup configurations at different stages of the BM@N experiment.

Year	2016	2017 Spring	2018 Spring	2022 Spring	2023	After 2023
Beam	d(↑)	C	Ar, Kr	Kr, Xe	Au	Au
Max.int., Hz	0.5M	0.5M	0.5M	0.5M	0.5M	2M
Trigger rate, Hz	5k	5k	10k	10k	10k	up to 50k
Cent.tracker status	6 GEM half-planes	6 GEM half-planes	6 GEM half-planes + 3 FwdSi	7 GEM full planes + 3 FwdSi	7 GEM full planes + 3 FwdSi + 2 STS	7 GEM full planes + 4 STS
Exp. staus	technical run	technical run	technical + physics	stage1 physics	stage1 physics	high rate stage 2 physics

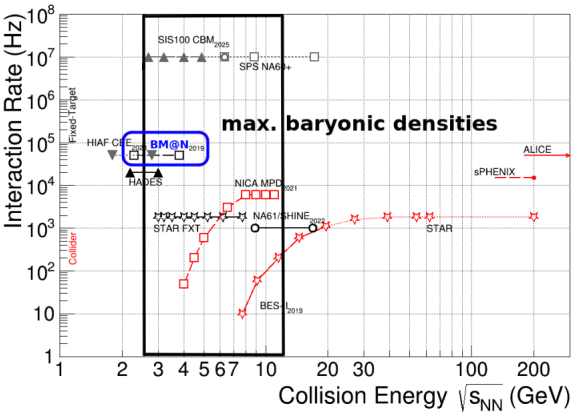

Fig. 2. Heavy ion experiments: interaction rate and nucleon-nucleon collision energy in c.m.s.

the energy range of the HADES experiment. The acquisition rate of non-peripheral collisions, i.e., central or intermediate interactions is expected to range from 20 to 50 kHz at the second stage of the BM@N experiment in 2022 and later. The interaction rate is limited by the capacity of the data acquisition system and readout electronics.

4.1. *Technical runs with deuteron and carbon beams*

Technical runs with the BM@N detector were performed in the deuteron beam in December 2016 and in the carbon beam in March 2017. The kinetic energy was 4 AGeV for the deuteron beam and was varied from 3.5 to 4.5 AGeV for the carbon beam. The configuration of the BM@N tracking system in these runs comprised a forward silicon strip plane, five GEM detectors with the size of 66 $\times$ 41 cm^2 and two GEM detectors with the size of 163 $\times$ 45 cm^2. The GEM detectors were combined into 6 GEM planes. The beam crossed the GEM detectors in the middle of the sensitive area. The experimental data from the central tracker, outer drift chambers, time-of-flight detectors, zero degree calorimeter and trigger detectors were read out using the integrated data acquisition system. The collected data were used to check efficiencies of sub-detectors and develop algorithms for the event reconstruction and analysis. In particular, experimental data of minimum bias interactions of the beam with different targets were analyzed with the aim to reconstruct tracks, primary and secondary vertices using the central tracking detectors.[28–31] The track reconstruction method was based on the so-called cellular automaton approach.[32] Since the GEM tracker configuration in the carbon run was tuned to measure relatively high-momentum beam particles, the geometrical acceptance for relatively soft decay products of strange V0 particles was rather low. The Monte Carlo simulation showed that only $\sim$ 4% of Λ hyperons and $\sim$ 0.8% of K^0s could be reconstructed. Λ hyperons were reconstructed using their decay mode

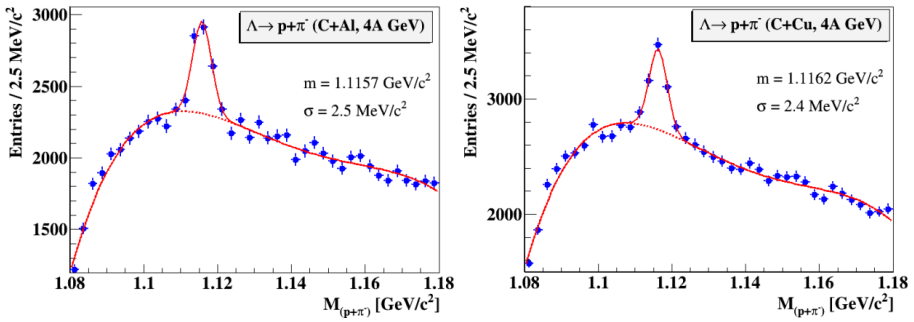

Fig. 3. Λ hyperon signals in the invariant mass spectrum of (p, π^-) pairs reconstructed in interactions of the 4 AGeV carbon beam with the Al,Cu targets.

into (p, π^-) pairs. Since particle identification at this stage of the analysis was not used, all positive tracks were considered as protons and all negative as π^-. The invariant mass distributions of (p, π^-) pairs are shown in Fig. 3 for reconstructed interactions of the carbon beam with the Al, Cu targets. In future experiments the background under the signal will be reduced by introducing additional silicon tracking detectors to improve the primary and decay vertex resolution.

4.2. *Technical run with argon and krypton beams*

The extended configuration of the BM@N set-up was realized in the next run with the argon and krypton beams performed in March 2018. The set-up comprised six planes of GEM detectors with the size of 163 × 45 cm^2, three forward silicon strip planes, outer tracker based on two drift chambers and a cathode strip chamber, full time-of-flight system consisting of ToF-400 and ToF-700, extended trigger system, hadron ZDC and electromagnetic ECAL calorimeters. The GEM tracking detectors covered only the upper half of the acceptance within the analyzing magnet.

In analogy with the analysis of the carbon beam data, Λ hyperons were reconstructed in argon-nucleus interactions using their decay mode into (p,π^-) pairs. Candidates to Λ decays were reconstructed as neutral V0 topologies without identification of the decay products. All positive tracks were considered as protons and all negative tracks as π^-. The Λ hyperon signal has a width sigma of 3–3.5 MeV for different targets, which is similar to the width of the Λ signal in carbon-nucleus interactions. Taking into account the momentum spectra of reconstructed p, π^- decay products, the 3–3.5 MeV Λ mass resolution corresponds to 2.5–3.5% momentum resolution for p, π^-. Figure 4 illustrates charged particles and nuclear fragments identifies with ToF-400 and ToF-700 systems in the run.

4.3. *Set-up upgrade for the first stage of physical program*

At the first stage of the experiment starting in spring 2022, three planes of the forward silicon detectors will be used in combination with seven planes of the GEM

detectors to reconstruct interactions of middle size ions (Kr, Xe) with fixed targets (Fig. 5).

The outer tracking system will be extended with four CSC $1 \times 1\ m^2$ and one CSC $1.5 \times 2.2\ m^2$. The efficiency of the $\Lambda \to p + \pi^-$ decay product reconstruction in the hybrid FwdSi + GEM tracker and signal of Λ hyperon in simulated interactions of the Xe beam with the kinetic energy 3.9 AGeV with the Sn target are shown in Fig. 6.

4.4. *Final configuration of the tracking system upgrade*

At the second stage of the BM@N experiment after 2023, four two-coordinate planes of the STS detectors will be installed in front of the GEM detectors instead of FwdSi detectors to improve track reconstruction in heavy ion collisions. Unlike FwdSi front-end electronics the STS front-end electronics is capable to register

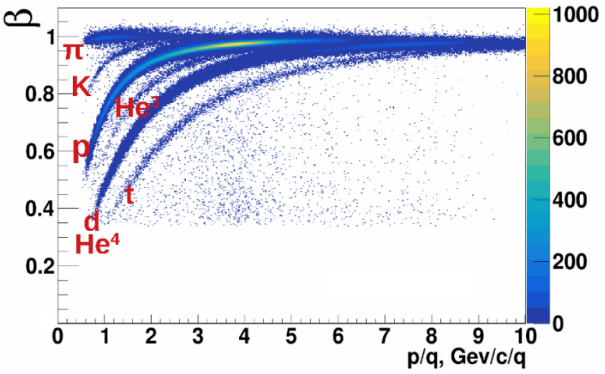

Fig. 4. Charged particles and nuclear fragments produced in interactions of 3.2 AGeV argon beam with the fixed targets and identified with ToF systems.

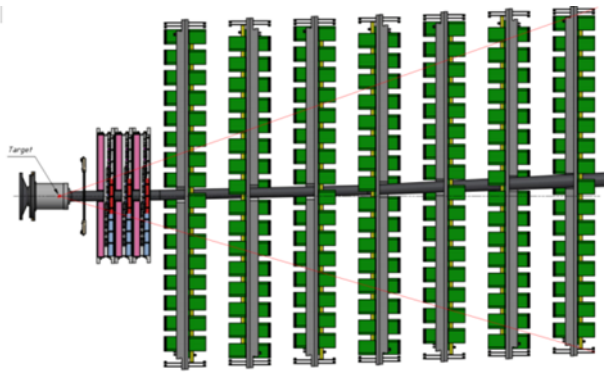

Fig. 5. Schematic view of the initial hybrid tracker based on 3 forward silicon planes and 7 GEM planes. The carbon vacuum beam pipe follows the trajectory of the beam.

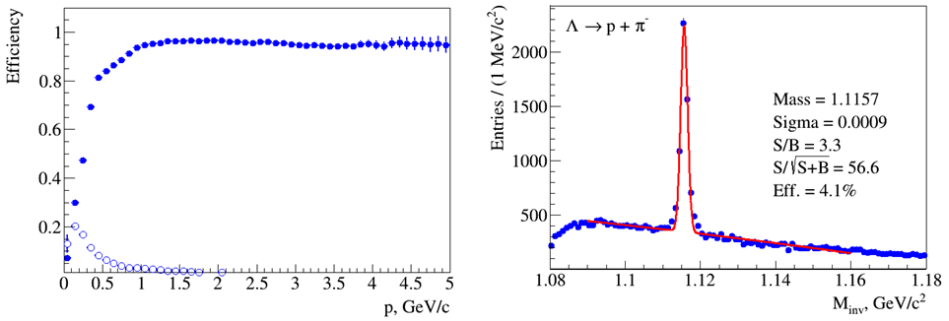

Fig. 6. Left plot: Efficiency of the Λ decay product (proton or π^-) reconstruction (filled symbols) and fake tracks (open symbols) as a functopn of momentum in the hybrid FwdSi + GEM tracker in simulated Xe + Sn interactions. Right plot: Signal of Λ hyperon in the invariant mass spectrum of simulated (p, π^-) reconstructed in the hybrid FwdSi + GEM tracker.

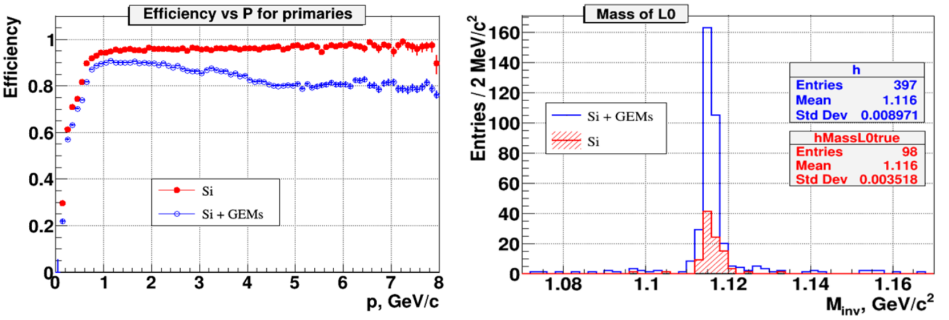

Fig. 7. Left plot: Efficiency of primary charge particle reconstruction in the hybrid STS + GEM tracker (blue histogram) and STS tracker alone (red histogram). Right plot: Reconstructed signal of Λ hyperon for the STS and STS + GEM tracker configurations.

interactions with the event rate of 50 kHz, which is the primary goal of the BM@N experiment (see Fig. 2). To record interactions with the 50 kHz rate, the front-end electronics of the GEM detectors should be upgraded to a faster version based on the VMM3a chips, which is presently under development. The STS + GEM tracking system was simulated to study its performance for reconstruction of hyperons and hypernuclei in interactions of heavy nuclei (up to Au + Au). The efficiency of reconstruction of primary charged particles is presented in Fig. 7(left) for the hybrid STS + GEM tracking system (blue histogram) and for the silicon STS stations alone (red histogram). Although the GEM detectors are less efficient in high multiplicity events due to lower granularity than the STS detectors, the STS + GEM tracking algorithm is able to reconstruct four times more Λ hyperons than the STS tracker alone (Fig. 7, right). The hybrid tracking system is also able to reconstruct cascade decays of Ξ^- hyperons to $\Lambda^+\pi^-$ and hypertriton nuclei ${}_{\Lambda}\mathrm{He}^3$ in the decay modes to $He^3 + \pi^-$ and $p + d + \pi^-$ with a similar efficiency.

5. Conclusions

The BM@N experimental set-up upgraded with hybrid tracking system and vacuum beam pipe will allow to perform measurements of multi-strange hyperons and light hypernuclei produced in heavy ion collisions at a trigger rate up to 50 kHz. The data achieved by the BM@N experiment in so far poorly studied Nuclotron energy range will help to shed light on QCD matter properties at high densities and temperatures.

Acknowledgments

This work was supported by the Russian Foundation for Basic Research (RFBR): grant No. 18-02-40036.

References

1. https://fair-center.de
2. https://nica.jinr.ru
3. CBM Collab (T. Ablyazimov *et al.*), *Eur. Phys. J. A* **53** (2017) 60.
4. V. Golovatyuk *et al.*, *Nucl. Phys. J. A* **982** (2019) 963.
5. BM@N Collab (M. Kapishin), *Nucl. Phys. J. A* **982** (2019) 967.
6. I. C. Arsene *et al.*, *Phys. Rev. C* **75** (2007) 24902.
7. A. Le Fevre *et al.*, *Nucl. Phys. A* **945** (2016) 112.
8. C. Pinkenburg *et al.*, *Phys. Rev. Lett.* **83** (1999) 1295.
9. P. Danielewicz, R. Lacey, W.G. Lynch, *J. Science* **298** (2002) 1592.
10. KaoS Collab (C. Sturm *et al.*), *Phys. Rev. Lett.* **86** (2001) 39.
11. Ch. Fuchs *et al.*, *Phys. Rev. Lett.* **86** (2001) 1974.
12. C. Hartnack and J. Aichelin, *J. Phys. G* **28** (2002) 1649.
13. F. Li *et al.*, *Phys. Rev. C* **85** (2012) 064902.
14. G. Graef *et al.*, *Phys. Rev. C* **90** (2014) 064909.
15. A. Andronic *et al.*, *J. Phys. G* **38** (2011) 124081.
16. P. Braun-Munzinger, J. Stachel and C. Wetterich, *Phys.Lett. B* **596** (2004) 61.
17. A. Andronic, P. Braun-Munzinger and J. Stachel, *Acta Phys. Polon. B* **40** (2009) 1005.
18. HADES Collab (G. Agakishiev *et al.*), *Eur. Phys. J. A* **47** (2011) 21.
19. H. T. Cromartie *et al.*, *Nat. Astron.* **4** (2020) 72.
20. W. Weise *JPS Conf. Proc.* **26** (2019) 011002.
21. A. Andronic *et al.*, *Phys. Lett. B* **697** (2011) 203.
22. A. S. Botvina *et al.*, *Phys. Lett. B* **742** (2015) 7.
23. BM@N Conceptual Design Report: http://nica.jinr.ru/files/BM@N/BMN-CDR.pdf.
24. F. Sauli *Nucl. Instr. Meth. A* **805** (2016) 2.
25. D. Baranov *et al.*, The Silicon Tracking System as Part of the Hybrid Tracker of the BM@N Experiment: Technical Design Report (2020) 101.
26. A. P. Byszuk *et al.*, *JINST* **12** (2017) C02061.
27. A. Galavanov *et al.*, *JINST* **15** (2020) C09038.
28. BM@N Collab (M. Kapishin), *Eur. Phys. J. A* **8** (2016) 213.
29. BM@N Collab (M. Kapishin), *Phys.Atom.Nucl.* **80** (2017) 1613.
30. BM@N Collab (M. Kapishin), *Nucl.Phys. A* **982** (2019) 967.
31. M. Kapishin, *JPS Conf. Proc.* **32** (2020) 010093.
32. I. Kisel, *Instrum. Meth. A* **566** (2006) 85.